Inverse lyotropic phases of lipids and membrane curvature

2006 J. Phys.: Condens. Matter 18 S1105

(http://iopscience.iop.org/0953-8984/18/28/S01)

INSTITUTE OF PHYSICS PUBLISHING JOURNAL OF PHYSICS: CONDENSED MATTER

J. Phys.: Condens. Matter **18** (2006) S1105–S1124 doi:10.1088/0953-8984/18/28/S01

Inverse lyotropic phases of lipids and membrane curvature

G C Shearman, O Ces, R H Templer and J M Seddon

Department of Chemistry, Imperial College London, SW7 2AZ, UK

E-mail: j.seddon@imperial.ac.uk

Received 13 March 2006
Published 28 June 2006
Online at stacks.iop.org/JPhysCM/18/S1105

Abstract

In recent years it has become evident that many biological functions and processes are associated with the adoption by cellular membranes of complex geometries, at least locally. In this paper, we initially discuss the range of self-assembled structures that lipids, the building blocks of biological membranes, may form, focusing specifically on the inverse lyotropic phases of negative interfacial mean curvature. We describe the roles of curvature elasticity and packing frustration in controlling the stability of these inverse phases, and the experimental determination of the spontaneous curvature and the curvature elastic parameters. We discuss how the lyotropic phase behaviour can be tuned by the addition of compounds such as long-chain alkanes, which can relieve packing frustration. The latter section of the paper elaborates further on the structure, geometric properties, and stability of the inverse bicontinuous cubic phases.

1. Introduction

In this paper we review previous work from our research group on those lyotropic liquid-crystalline phases of lipids that exhibit *inverse* interfacial curvature. The most common and best characterized of these are the inverse bicontinuous cubic phases $Ia3d$, $Pn3m$ and $Im3m$ [1–4], the inverse hexagonal H_{II} phase [5, 6], and the inverse micellar cubic $Fd3m$ phase [7]. We will describe the development of our understanding of the role of curvature elastic energy, along with packing constraints, in stabilizing these inverse phases [8–14]. We will not deal with the kinetics or the mechanisms of transitions between inverse phases, as we have recently covered these topics elsewhere [15–17].

The human body contains of the order of 10^{13} cells, each of which is spatially defined by a complex network of membranes that encapsulate and serve to compartmentalize numerous biological structures such as the cell itself, the endoplasmic reticulum, the Golgi apparatus, the mitochondria and the nucleus. It is well documented that the fluid bilayer structure of all biological membranes basically arises from the self-assembly properties of amphiphilic lipids

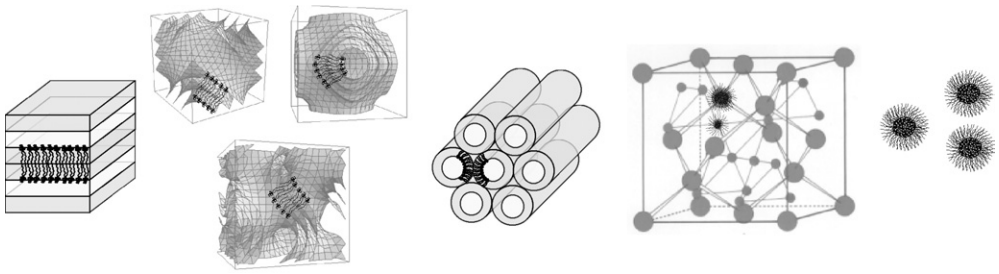

Figure 1. Schematic sketches of the most common inverse phases lying between the flat fluid lamellar L_α phase and the inverse micellar solution L_2, in order of increasingly negative interfacial mean curvature from left to right: inverse bicontinuous cubic (spacegroups $Pn3m$, $Im3m$, $Ia3d$), inverse hexagonal H_{II}, and inverse micellar cubic (spacegroup $Fd3m$).

in aqueous solution, driven by the hydrophobic effect. Embedded within or attached to the fluid bilayer is a diverse range of membrane proteins (e.g. receptors, ion channels, etc) that carry out a wide range of functional roles. This fluid mosaic model has been extended in the last decade to allow for the formation of membrane microdomains, particularly in the presence of sterols, sphingolipids, and certain glycoproteins, thought to have vital roles in a diverse range of functions such as trafficking and cell signalling. However, there are also many situations where the bilayer structure must be locally and temporarily destabilized, for example, during membrane fusion [18], and indeed there are many regions within cells where the membrane is quite highly curved. Biophysicists have been exploring the possible roles of curvature and lipid polymorphism in biological systems for some years already [19–21], but it is only very recently that membrane curvature, and its implications for static and dynamic processes in membrane structure and function, has emerged as a hot area of membrane biology [22–24]. Related to this is the question of bilayer asymmetry in lipid composition [25], since this is one way of inducing membrane curvature. However, even symmetric lipid bilayers may develop a tendency for *monolayer* curvature, depending on the thermodynamic conditions (temperature, pressure, pH, salt concentration, hydration, osmotic pressure, etc). If the desire for interfacial curvature towards the aqueous region becomes sufficiently strong, a transition will tend to occur from the fluid bilayer lamellar phase to an inverse phase, where there is a negative monolayer interfacial mean curvature. There is a considerable amount of microscopy data which supports the idea that inverse lipid phases (hexagonal and/or cubic) can occur within certain cells [19]. Inverse lipid phases may also be useful for biotechnological applications [26], such as *in cubo* crystallization of membrane proteins [27–29], drug delivery [30], and DNA/lipid complexes for gene therapy [31, 32].

A range of inverse phases can be formed by lipids when placed in contact with water [33], and these are illustrated in figure 1. The fluid lamellar phase, L_α, can be visualized as a set of flat bilayer sheets stacked on top of each other and forms the basic building block of all biological membranes. In the inverse micellar phase, L_2, the hydrophilic headgroups are arranged around water cores, with the hydrophobic chains extending outwards. The inverse micelles have a disordered packing, with only local positional correlations and no long-range order. The inverse hexagonal phase, H_{II}, can be visualized as a set of hexagonally packed cylinders, where water channels pass through the core of each cylinder. More complex mesophases such as the inverse bicontinuous cubic phases (Q_{II}) [34] may also arise that display three-dimensional periodicity (non-cubic phases of rhombohedral or tetragonal symmetry have also been observed, although only rarely). The most common such cubic phases are of crystallographic spacegroups $Im3m$,

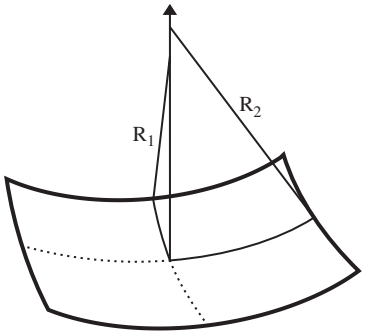

Figure 2. The principal curvatures at one point on a monolayer, where $c_1 = 1/R_1$ and $c_2 = 1/R_2$.

$Pn3m$ and $Ia3d$. In all three cases, water channels weave their way through a single continuous bilayer that divides space equally into two inter-linked but separate aqueous sub-volumes. Finally, the discontinuous inverse micellar cubic phase, of spacegroup $Fd3m$, consists of two different sizes of quasi-spherical micelles, arranged on a face-centred cubic lattice [35]. The phases depicted in figure 1 have been arranged according to their average *interfacial mean curvature*, a concept that is discussed in greater detail during the course of this review.

1.1. Interfacial curvature

Consider a single flat lipid monolayer. Varying the thermodynamic parameters of this system will tend to change the shape of the monolayer. For instance, in the absence of any constrictions, an increase in temperature would lead to the chains of the lipids splaying out away from each other, and would generate a curved configuration. For any given point on the monolayer, a normal to the surface can be extended, and the principal curvatures, c_1 and c_2, can be obtained as illustrated in figure 2, as the maximum and minimum values of curvature respectively.

The two principal curvatures are perpendicular to each other and, when combined as a sum or a product, give the mean curvature H or the Gaussian curvature K at that point:

$$\begin{aligned} H &= 1/2\,(c_1 + c_2) \\ K &= c_1 c_2. \end{aligned} \tag{1}$$

Conversely, if both the mean and Gaussian curvatures are known as a function of position, the shape of the surface is determined. A flat surface has zero mean and zero Gaussian curvature; if rolled into a cylinder or a cone, its mean curvature will change, but its Gaussian curvature will remain zero. In fact, it is impossible to alter the Gaussian curvature of a surface by bending alone; some distortion, such as stretching, compression or tearing, must occur. Thus, for example, a flat surface cannot be wrapped into a spherical shape (which has a positive Gaussian curvature), without some stretching or creasing occurring. Similarly, it cannot be deformed into a saddle surface (which has a negative Gaussian curvature) without some distortion.

One source of confusion in treating membrane curvature is the *sign* of the monolayer mean curvature. We adopt the convention (figure 3) that *positive* mean curvature corresponds to the monolayer bending towards the hydrocarbon chain region and away from the water region, and *negative* mean curvature is when the bending is the other way round. Thus the spontaneous monolayer mean curvature of all inverse curved phases should always be negative (note that some authors [19] adopt the opposite convention). Positive mean curvature tends to be favoured

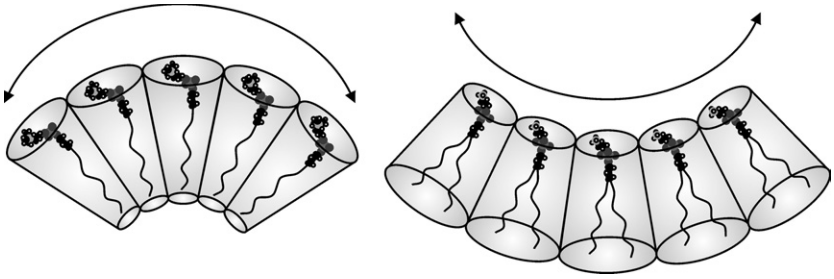

Figure 3. Convention adopted for positive and negative (inverse) mean curvature of a lipid monolayer, shown on the left and right, respectively.

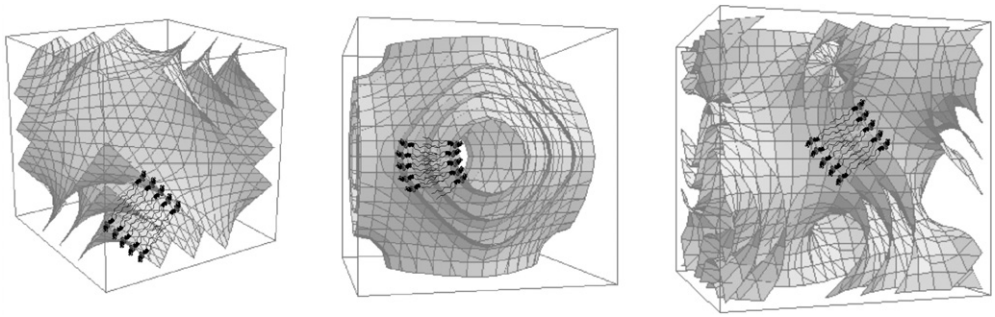

Figure 4. The three minimal surfaces, D, P, and G (gyroid), which sit at the bilayer mid-plane and underlie the bicontinuous cubic phases $Pn3m$, $Im3m$, and $Ia3d$.

by cone-shaped amphiphiles (designated as type I), and negative mean curvature by wedge-shaped amphiphiles (type II).

Saddle surfaces where the principal curvatures are equal in magnitude (and opposite in sign) have zero mean curvature at all points, and are known as *minimal surfaces*. Such surfaces can be extended to fill space periodically, forming *infinite periodic minimal surfaces* (IPMS). These porous surfaces have constant (zero) mean curvature at all points, but continuously varying Gaussian curvature, which is everywhere non-positive, varying between a most negative value at saddle points and zero at flat points. Such mathematical surfaces were hypothesized by Scriven in 1976 [36, 37] to describe the underlying physical interfaces observed in certain ternary microemulsion mixtures of oil, surfactant and water. This concept has subsequently been shown to be relevant to the geometric description of many self-assembled phases of amphiphilic molecules, such as the bicontinuous cubic phases, as well as other self-assembled soft matter such as block copolymers [38]. For the inverse cubic phases $Im3m$, $Pn3m$ and $Ia3d$, the bilayer mid-plane has been shown to sit on the P, D, and G (gyroid) minimal surfaces respectively (figure 4), leading to the alternative naming as Q_{II}^{P}, Q_{II}^{D}, and Q_{II}^{G}, respectively, for these three cubic phases. These three minimal surfaces can be interconverted by a 'Bonnet' transformation [39], a mathematical procedure that performs a one-to-one mapping between equivalent surface patches on the three surfaces, thereby preserving the same distribution of Gaussian curvature (and zero mean curvature) at all points. Although the three minimal surfaces have the same area per unit cell, they fill space to different degrees of compactness (see section 2.5).

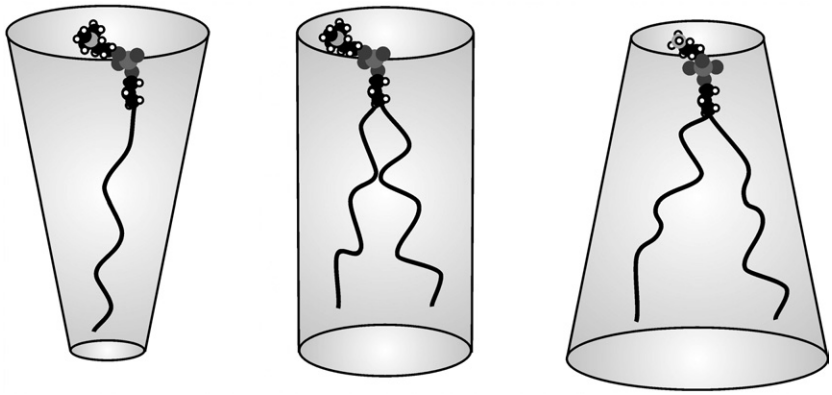

Figure 5. The 'shape' of amphiphiles as determined by their packing parameter S, where the cone (left) has $S < 1$, $S = 1$ for the cylindrical shape (centre) and the inverted cone-shape (right) is preferred by lipids with $S > 1$.

1.2. Lipid packing parameters and phase preferences

The lipids that can form these curved inverse phases tend to have certain structural similarities. Israelachvili *et al* [40] suggested that the lipids can be usefully categorized by their 'shape' or 'packing parameter', S, which subsumes the basic geometric parameters, given by:

$$S = \frac{v}{a_0 l_C} \tag{2}$$

where a_0 is the optimum surface area of the headgroup, l_C is the maximum length of the chains, and v is the molecular volume of the chains. Israelachvili and co-workers showed that, in a qualitative sense, the shape of the aggregates formed by any lipid in contact with water was related to its packing parameter (figure 5). A typical example would be lysophosphatidylcholine, which is a single-chained lipid, where $1/3 < S < 1/2$ [41]. A lipid with this packing parameter would tend to be cone-or wedge-shaped, and it will tend to form positively curved micellar aggregates. Lyotropic mesophases adopted by such aggregates are known as type I, or 'normal', phases. In this paper we have focused on 'inverse', or type II, lipid phases, which are formed by lipids with $S > 1$, and which are hence inverted cone-shaped. Such lipids are typically characterized by having a small headgroup cross-sectional area relative to that of the chain region (e.g. double-chained species that cause the tail-region to splay out relative to the headgroup region).

1.3. Lipid membrane energetics

Although the model detailed by Israelachvili and co-workers illustrates very simply why the flat bilayer membrane may not always be the aggregate shape of choice, it fails to predict the appearance of the inverse bicontinuous phases, which are prevalent in the phase behaviour (when measured in isolation) of many phospholipids and glycolipids found in cell membranes. Because of this, more rigorous approaches have been developed, which consider the total free energy of the system, consisting of assemblies of lipid and water molecules. Gruner *et al* [42] assumed that the free energy would be dominated by four factors: the membrane curvature elasticity, g_C; the packing of the hydrocarbon chains, g_P; the hydration force; and lastly the electrostatic contributions. This model was refined later to include any other interactions, which were grouped together with the hydration and electrostatic forces into a single free-

energy interaction term, g_{inter}. This resulted in the total free energy of the system being given as:

$$g_{\text{tot}} = g_{\text{C}} + g_{\text{P}} + g_{\text{inter}}. \tag{3}$$

The final term in this expression is usually assumed (or arranged experimentally) to be negligible, leaving the curvature elasticity and the packing of the hydrocarbon chains as the chief terms dictating the free energy of the system.

2. Membrane curvature elasticity

The curvature elasticity of lipid membranes had previously been considered by Helfrich [43], who simplified the problem by reducing the lipid bilayer to an infinitely thin elastic surface, which could then be treated mathematically. Deformation of the surface would then have an associated energy cost dependent only on any changes of the curvature of the surface, defined by its mean curvature, H, and its Gaussian curvature, K. The energy costs per unit area of such deformations are then given by the bending modulus, κ, and the Gaussian modulus, κ_{G}, which describe the energy required to bend the surface (change its mean curvature) and to change its Gaussian curvature [43, 44]. The latter quantity only has significance for the area-integrated energy when there is a change in topology of the membrane (this is a consequence of the Gauss–Bonnet theorem). These two moduli were combined into the 'Helfrich ansatz', which gives the curvature elastic energy per unit area, g_{C}, for a membrane as:

$$g_{\text{C}} = 2\kappa(H - H_0)^2 + \kappa_{\text{G}}K \tag{4}$$

where H_0 is the mean curvature of the surface when totally relaxed (often referred to as the *spontaneous mean curvature*). Note that this expression is quadratic in the principal curvatures; the possibility of extending it to terms in the fourth power of the principal curvatures has also been considered [45].

The spontaneous mean curvature H_0 is determined by the distribution of lateral stresses that occurs across the actual lipid monolayer. Recollecting the illustration used earlier of a double-chained phospholipid monolayer, it is clear that the lateral forces acting at the headgroup region will not equal those at the polar–apolar interface or the tail–tail interactions. The forces at the interfacial region are dominated by the interfacial tension, resulting from the hydrophobic effect that acts to minimize contact between water and the hydrophobic chain region, i.e. the interfacial tension is an attractive force, which tries to pack the amphiphiles tightly together within a monolayer. Counterbalancing this are the overall repulsive pressures within the headgroup and chain regions. The repulsive force between the chains is due to thermally activated *trans–gauche* conformational changes, and this will therefore increase with increasing temperature. In contrast, an increase in pressure would favour more *trans* conformations, thereby allowing the chains to pack closer together laterally. There are several contributions, such as electrostatic, steric and hydration interactions, to the repulsive headgroup pressure (there may also be weaker attractive interactions due to residual headgroup–headgroup hydrogen-bonding). Figure 6 is a schematic representation of a lateral stress profile, which shows the lateral stress, $t(z)$, as a function of the distance, z, through an amphiphilic monolayer.

For the monolayer to be at its equilibrium area, the integral of the lateral stress across the monolayer, $\int t(z)\,\mathrm{d}z$, should be zero. The spontaneous mean curvature is proportional to the first moment of the lateral stress across the monolayer, $\int zt(z)\,\mathrm{d}z$, and is expected to be *negative* for amphiphiles with small polar headgroups [46]. Although for such a monolayer, H_0 may be negative, when two identical monolayers are placed back-to-back the spontaneous mean curvature for the bilayer, H_0^{b}, must be zero to prevent the formation of otherwise energetically

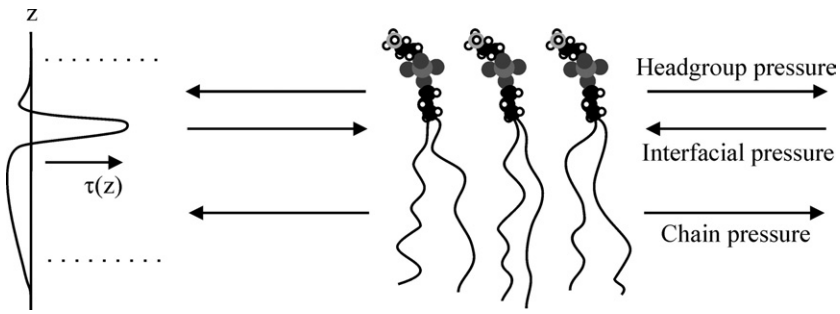

Figure 6. A schematic lateral stress profile across a lipid monolayer.

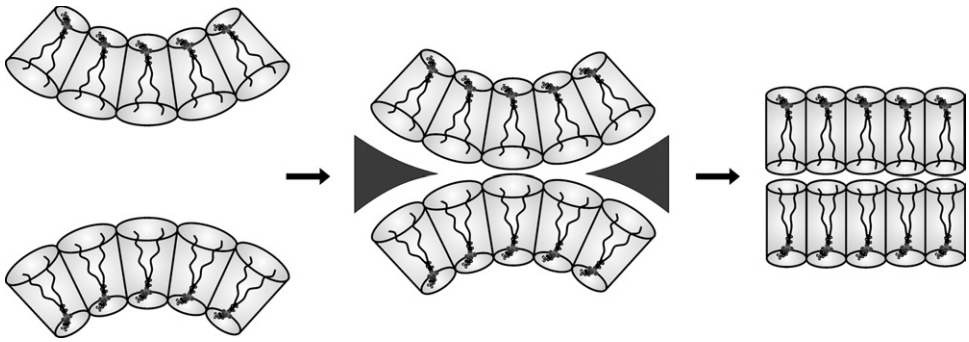

Figure 7. Curvature frustration illustrated for the case of a symmetric bilayer consisting of two monolayers that have an inherent desire to bend. In order to avoid energetically unfavourable voids, the two monolayers must lie flat back-to-back, resulting in a stored curvature elastic stress.

costly voids, as illustrated in figure 7. Note, however, that this does not hold true for an *asymmetric* bilayer, such as a real cell membrane, where the two halves of the bilayer need not be in balance, leading to a tendency for the bilayer to curve.

When the desire to form a phase having curved interfaces is not very great, the bilayer will remain as a flat structure, i.e. in the lamellar phase, albeit slightly thinner than its conformationally preferred thickness. This stored curvature elastic energy translates into the bilayer expanding laterally and the headgroup area increasing above its preferred value. However, this effect can only be tolerated up to a certain point, due to the high energetic cost of exposing the hydrocarbon chains to water (the hydrophobic effect). Upon further stressing the layers, a transition to an inverse phase may be induced, where the interface can bend towards the aqueous region, allowing the headgroup area to decrease and the chains to splay out further. It has been suggested that certain membrane proteins may release stored curvature elastic stress locally [47–49] during insertion into the bilayer by allowing the chains to splay more and forcing the headgroups together, which is energetically favourable.

2.1. Determination of the curvature elasticity of inverse curved phases

Experimentally, it is possible to measure the curvature elasticity of curved inverse phases of lipids. The simplest parameter to obtain is the spontaneous mean curvature H_0. A decision has to be made as to where to place the surface with respect to which the curvature and the

elastic parameters will be defined. The simplest is to choose the *pivotal surface*, defined as the surface at which there is no change in the molecular cross-sectional area upon bending; alternatively one can choose the *neutral surface*, where bending and stretching deformations are energetically decoupled [50, 51]. For the inverse hexagonal H_{II} phase, the pivotal surface typically lies just on the hydrocarbon chain side of the polar headgroup region. It was recognized two decades ago by Gruner and co-workers [52] that the addition of an oil, typically an alkane, to a lipid–water system that has a propensity to form inverse phases will relieve the packing frustration energy (see section 3) characteristic of inverse hexagonal phases, by partitioning into the hydrophobic interstices. Templer *et al* [14] adopted the approach of using a long-chain alkane or alkene, such as tricosane or 9-*cis*-tricosene, in order to minimize permeation into the lipid chain region. In fact, it was found to be preferable for the added hydrocarbon to be fluid, i.e. unsaturated, thereby avoiding the added energy costs involved in melting the alkane. Addition of the hydrocarbon to the lipid, in excess water conditions, will progressively relieve packing frustration, eventually forming the inverse hexagonal phase, where characterization of the phase, as well as determination of the lattice parameter, is done using x-ray diffraction. With further addition of the hydrocarbon, the lipid–water system will continue to swell, until a limiting point is reached. The ratio of lipid to hydrocarbon at this limiting point is then kept constant while the water composition, n_w, is varied, and the lattice parameter measured. Since the Gaussian curvature for cylindrical surfaces is zero, the curvature elasticity is only dependent on the monolayer bending modulus κ. Initially, the system will swell, but at some water concentration the inverse hexagonal phase will not swell any further and will reach a constant lattice parameter, the value of R_P at the excess water point then yielding the spontaneous radius of curvature, R_0, and hence the spontaneous mean curvature of the inverse hexagonal phase from the relationship $H_0 = 1/(2R_0)$.

The osmotic stressing technique can be used to obtain the bending modulus of a curved inverse hexagonal or bicontinuous cubic phase [53–55]. Here, a lipid sample is placed in contact with a polymer solution, typically a polyethylene glycol solution, either inside a semi-permeable membrane or directly into the solution. The osmotic pressure, π, of the polymer solution dehydrates the lipid mesophase until equilibrium is achieved, and is effectively a measure of the bending energy of the system, since the monolayer mean curvature changes in magnitude (become more negative) as the aqueous channels of the phase shrink. Repetition over a range of osmotic pressures and fitting (for the H_{II} phase) allows the bending modulus κ to be determined.

Finally, the monolayer Gaussian curvature modulus for a bicontinuous cubic phase can also be estimated, as illustrated by Templer *et al* [13], although the results are only valid for studies on inverse bicontinuous cubic phases that are relatively highly swollen [10]. This ensures that the assumption that the bending energy of the monolayer is subject only to curvature variations, introduced in the Helfrich ansatz, holds true. As with the spontaneous mean curvature, the ratio of the Gaussian (saddle-splay) modulus to the bending modulus, κ_G/κ, is determined by measurements of the swelling of the inverse cubic phase. As before, the energy minimum occurs at the excess water point, and κ_G/κ can then be ascertained. The associated equations and their derivations are described by Templer *et al* [13].

Siegel and Kozlov [56] have recently pioneered an alternative technique to measure this ratio, which exploits the fact that, at the L_α–Q_{II} phase transition, the bilayer Gaussian modulus is equal to zero. The ratio of the elastic moduli can then be simply expressed (equation (5)) as a function of the spontaneous mean curvature at the temperature of the transition, T_Q, together with the distance from the bilayer mid-plane to the neutral surface of the monolayer, δ. The drawback of this method is that it relies on the L_α–Q_{II} transition being sharp, which is not necessarily the case:

Table 1. The expected signs of the monolayer and bilayer spontaneous curvatures and elastic moduli for 'inverse phase-forming' lipids.

	Monolayer	Bilayer
H_0	−ve	0
κ	+ve	+ve
κ_G	−ve	+ve

$$\left.\frac{\kappa_G}{\kappa}\right|_{T_Q} = 2H_0(T_Q)\delta. \tag{5}$$

2.2. Monolayer versus bilayer curvature elastic parameters

It is important to emphasize that the curvature elastic parameters acquired experimentally, using the techniques mentioned in the previous section, are all related to the curvature of a monolayer, rather than a bilayer, for which any variables will be denoted here by a superscript b. The relationship between the spontaneous mean curvature of a monolayer, H_0, and a bilayer, H_0^b, has been highlighted previously and, for symmetric bilayers, H_0^b should be zero. In considering the *bilayer* bending modulus, κ^b, the energy required to bend two sheets should be twice that needed to bend only one sheet. This implies that κ^b should have a value that is simply twice that of the monolayer bending modulus, κ. However, a more complex situation exists when considering the link between the monolayer and bilayer Gaussian moduli, κ_G and κ_G^b [57]. The latter is directly related to the monolayer Gaussian modulus, but also includes a term that contains the bending modulus κ. The explicit expressions for the *bilayer* curvature parameters are:

$$\begin{aligned} H_0^b &= 0 \\ \kappa^b &= 2\kappa \\ \kappa_G^b &= 2\,(\kappa_G - 4\kappa H_0 l) \end{aligned} \tag{6}$$

where the bilayer is taken to be symmetric, and l is the monolayer thickness. The bending modulus κ is *positive* for both the monolayer and bilayer cases (table 1). However, the situation is more complicated for the Gaussian modulus κ_G. The monolayer Gaussian modulus has been predicted to be *negative* for systems forming inverse curved phases, and with a magnitude less than that of the bending modulus κ [13]. This reflects the fact that a uniform monolayer with a negative H_0 would prefer to develop a spherical curvature, i.e. a *positive* K. However, the second term in equation (6) for κ_G^b will tend to make the *bilayer* Gaussian modulus κ_G^b *positive*, since H_0 is negative in this case, and, inserting typical values for κ, H_0 and l, the second term is expected to be larger in magnitude than the first term.

We now consider the magnitude of each of these parameters, to facilitate a more complete understanding of the nature of curvature elasticity for the curved inverse phases of lipids. Recently, Zimmerberg and Kozlov [23] published a list of the effective spontaneous curvatures for a series of lysophospholipids and other lipids, obtained from a range of different sources. The values range between around -0.05 to -1 nm^{-1} for the type II lipids given, but a typical value would be ~ -0.17 nm^{-1} for dioleoylphosphatidylethanolamine (DOPE) [54]. There has also been a significant amount of research [58–60] undertaken to elucidate the elastic moduli, though this has been focused mainly on the bending modulus (table 2). This was not purely due to the relative ease of determination of the bending modulus, but also because it was often

Table 2. Typical values of monolayer bending moduli κ for various fluid-phase lipids.

Lipid	κ/J	κ/k_BT	Reference
Dioleoylphosphatidylethanolamine (DOPE)	4.5×10^{-20}	11	[58]
Dioleoylphosphatidylcholine (DOPC)	3.7×10^{-20}	9	[58]
Dilauroylphosphatidylcholine (DLPC)	4.6×10^{-20}	11	[59]
Stearoyloleoylphosphatidylcholine (SOPC)	6.4×10^{-20}	15.5	[59]
Dimyristoylphosphatidylcholine (DMPC)	6.5×10^{-20}	15.8	[60]
1-monoolein (1-MO)	1.2×10^{-20}	2.9	[14]

Table 3. Typical values determined for the ratio of the monolayer elastic moduli.

Lipid	κ_G/κ	Reference
Monomethyl-dioleoylphosphatidylethanolamine	−0.83	[56]
1-MO/DOPC/DOPE	−0.75	[13]
2:1 lauric acid/dilauroylphosphatidylcholine	−0.70	[63]

(incorrectly!) assumed that the contribution of the Gaussian curvature energy to the free energy of a lipid system was too small to have any real significance.

The value of bending modulus for 1-monoolein (1-MO) is typical of monoacyl systems, and is much lower than values for the diacyl phospholipid systems. The fact that it is of the order of the thermal energy at room temperature, $k_BT \sim 4 \times 10^{-21}$ J, implies that 1-MO may exhibit considerable thermal bending fluctuations, even when considered as a bilayer. Phospholipid systems have significantly higher monolayer bending moduli, and so their persistence lengths, $\zeta = l \exp(2\pi\kappa/k_BT)$ [61] (where l is the dimension of an individual lipid molecule), are much greater than for the monoacyl systems. Short persistence lengths, such as those for monoacyl systems or even phospholipid bilayers doped with single-chain amphiphiles, imply that such lipid membranes will be more prone to rupturing, or micellar budding, than their pure phospholipid counterparts.

Theoretically, the ratio of the monolayer Gaussian curvature modulus to the bending modulus was predicted to lie within the range $-2 \leqslant \kappa_G/\kappa \leqslant 0$ for the bicontinuous cubic phases [62]. Templer *et al* have shown that there is an added restriction from the inference that compression of hydrocarbon chains will cause increased splay [13], which means that the ratio of the elastic moduli will lie within smaller bounds, $-1 \leqslant \kappa_G/\kappa \leqslant 0$. Experimentally obtained data (table 3) has been found to agree with this prediction.

2.3. The dependence of the curvature elasticity on temperature and pressure

The curvature elastic parameters are all affected by changes in the temperature or pressure, as mentioned earlier for the spontaneous mean curvature of a monolayer. Qualitatively, an increase in temperature will induce a higher degree of chain splay, therefore increasing H_0, whereas an increase in pressure will have the opposite effect. These effects are clearly seen in the temperature-dependent decrease, and pressure-dependent increase, in lattice parameter for inverse bicontinuous cubic phases [64, 65]. The latter effect is greatest in the presence of excess water, which facilitates the swelling of the lattice parameter by partitioning from the bulk into the cubic phases, in response to the application of hydrostatic pressure.

The monolayer bending modulus κ, and accordingly the bilayer bending modulus κ^b, should tend to decrease with increasing temperature, since the lipid layers will tend to expand laterally and thin transversely with heating [66]. However, apparent exceptions to this

behaviour have been reported [67]. Similarly, the bending modulus is expected to increase with hydrostatic pressure, and this is confirmed by recent neutron experiments on amphiphilic monolayers in a microemulsion system [68].

Much less is known about the effect of temperature and pressure on the Gaussian modulus, κ_G. The Gaussian curvature modulus is given by the second moment of the lateral stress profile $t(z)$ [44, 69]:

$$\kappa_G = \int_0^l t(z)(z-\xi)^2 \, dz \tag{7}$$

where ξ is the distance to the pivotal surfaces from the chain termini. Increasing the temperature is likely to have repercussions across the whole lateral stress profile, such as increasing the magnitude of the chain repulsions. The likelihood is that the magnitude of the monolayer Gaussian curvature modulus will decrease, and vice versa for an increase in pressure. An even more knotty problem is the effect of temperature or pressure on the *bilayer* Gaussian modulus κ_G^b, as the effects of four variables in equation (6), all of which are dependent on temperature and pressure, need to be incorporated. The fact that pressure has been shown to induce intermediate inverse bicontinuous cubic phases in a phospholipid system, which at 1 atm exhibits a direct L_α–H_{II} transition [64], implies that, at least in that case, pressure was increasing κ_G^b.

2.4. Relative stabilities of the bicontinuous cubic phases

The curvature energy of the bicontinuous cubic phases, expressed by the Helfrich equation (equation (4)) has normally been examined with reference to the monolayer thickness being nearly constant, i.e. the distance from the mid-bilayer minimal surface to the neutral or pivotal surface, ξ, is kept constant over the whole of the unit cell. For such parallel surfaces, their mean and Gaussian curvatures H^ξ and K^ξ, and area element dA^ξ, are related to the Gaussian curvature K and the area element dA on the minimal surface by noting that the two principal curvatures are changed from $c_1 = -c_2 = R^{-1}$ on the minimal surface (where R is its radius of curvature) to $c_1^\xi = (R+\xi)^{-1}$ and $c_2^\xi = -(R-\xi)^{-1}$ on the parallel surface. This leads directly to the following relations [21]:

$$\begin{aligned} H^\xi &= \frac{K\xi}{1+K\xi^2} \\ K^\xi &= \frac{K}{1+K\xi^2} \\ dA^\xi &= dA[1+K\xi^2]. \end{aligned} \tag{8}$$

These relations show that the geometric properties of the interface are dependent only on the Gaussian curvature of the underlying minimal surface and the distance ξ of the parallel surface from the minimal surface. They show that, because K is negative, the mean curvature of the parallel surface is *negative*, and its Gaussian curvature is *more negative* than the underlying minimal surface. Concomitantly, the area element (area per molecule) is *maximal* on the minimal surface and decreases with ξ. Relating this back to the Helfrich equation implies that the bicontinuous cubic phases should be energetically degenerate when the underlying minimal surfaces have the same area. The three bicontinuous cubic phases might therefore be expected to co-exist, a phenomenon that is only very rarely seen (and which might contravene the Gibbs phase rule). This implies that other interactions break the degeneracy of the Q_{II} phases, and possible explanations for this are discussed later. The experimental phase diagram shown in figure 8 for the 2:1 lauric acid/dilauroylphosphatidylcholine system shows that the bicontinuous cubic phases appear with increasing hydration in the order G → D → P, a sequence that

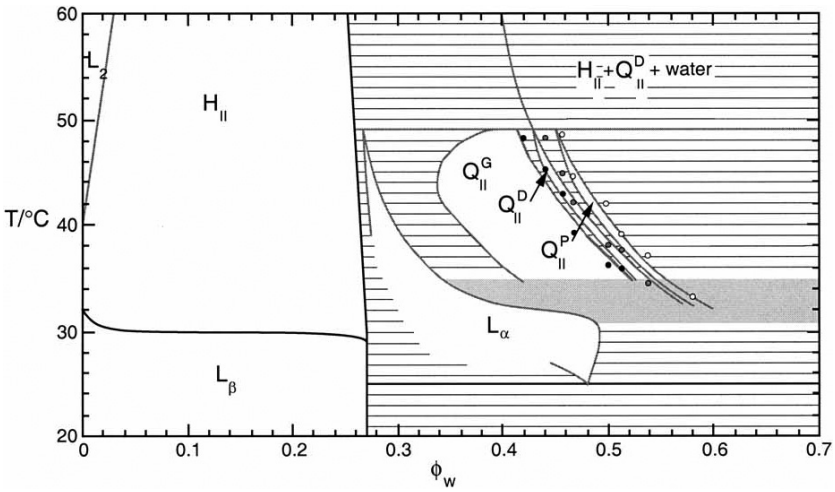

Figure 8. Experimental phase diagram of the 2:1 lauric acid/dilauroylphosphatidylcholine system, showing the progressive formation of the three inverse bicontinuous cubic phases $Ia3d$, $Pn3m$ and $Im3m$ with increasing water content (from [72]).

appears to be universal, although not all three bicontinuous cubic phases necessarily occur for a given lyotropic system.

An example of this is frequently given by the 1-monoolein/water system, in which only the $Ia3d$ and $Pn3m$ phases are seen (albeit in the sequence G → D). Larsson [70] justified this by examining the geometric constraints of each of the three Q_{II} phases. The inherent shape of the $Im3m$ phase seen in figure 1, which has narrow necks of the lipid bilayer through which the water channels pass, implies that, at a low water volume fraction, the necks will close up, as the bilayer itself possesses a certain thickness. This explanation was also applied to the $Pn3m$ phase, since it also suffers from the same geometric constraint, though to a lesser degree, allowing it to exist at lower water volume fractions than the $Im3m$ phase. However, for those water volume fractions at which all of the phases are expected to exist, experimental results demonstrate that this is not true, and one Q_{II} phase dominates. This implies that the three bicontinuous cubic phases cannot be energetically degenerate, and must have different curvature elastic energy or packing frustration, or some other interaction. Schwarz and Gompper [71] have shown that the free-energy density for a phase is dependent on the 'topological index' (a mathematical construct that is related to the porosity of a phase) which in turn can predict the phase sequence seen in figure 8.

Another interesting point to note is that the inverse bicontinuous cubic phases tend to be *more* hydrated than the fluid bilayer phase, even though they have an *inverse* interfacial curvature. This behaviour is also seen for many other lyotropic systems, and implies that the additional water is not tuning the preferred curvature of the interface (which would tend to prevent inverse phase formation), but is rather inertly filling the aqueous 'chambers' of the cubic phases, allowing the already fully hydrated interface to express its existing preferred negative interfacial curvature.

2.5. Geometric characteristics of the 'genus-3' bicontinuous cubic phases

The three inverse bicontinuous cubic phases have, up to this point, been discussed collectively, and their structures were only briefly touched upon with reference to their space group

Table 4. Geometric characteristics of the 'genus-3' inverse bicontinuous cubic phases.

Minimal surface	Cubic phase	g	χ	σ	V/V_{IPMS}	S/S_{IPMS}	a/a_{Pn3m}
D	$Pn3m$	2	−2	1.9189	0.5	0.5	1
P	$Im3m$	3	−4	2.3451	1	1	1.279
G	$Ia3d$	5	−8	3.0915	2	2	1.578

symmetry. However, this alone is unable to describe each structure uniquely, since a series of different morphologies may exist for each space group [73] and must be stated in conjunction with the topology of each of the three inverse bicontinuous cubic phases. In fact, although only the 'genus-3' D, P and G minimal surface cubic phases have ever been observed for lipid/water systems, there is a range of other cubic minimal surfaces that exist [74]. Schwarz and Gompper [71] modelled the distribution of the Gaussian curvature over a minimal surface for seven possible inverse bicontinuous cubic structures. The three inverse bicontinuous cubic phases were shown to have smaller widths for their respective Gaussian curvature distributions (which is the same for the D, P and G phases, since they are related to each other by the Bonnet transformation), leading to an enhanced stability of these phases, due to a lower frustration.

The *genus*, g, of a surface is topologically related to its connectivity. The periodic minimal surfaces D, P and G all have a genus of 3 for each topological unit cell [75]. The Euler–Poincaré characteristic, χ, is related to the genus of a surface, g, via $\chi = (2-2\mathrm{g})$, and hence has a value of $\chi_{\mathrm{IPMS}} = -4$ for these three minimal surfaces. The Gauss–Bonnet theorem states that the integrated Gaussian curvature over the area S_{IPMS} of the minimal surface unit cell is directly related to the Euler–Poincaré characteristic via $\int K \, \mathrm{d}S = 2\pi \chi_{\mathrm{IPMS}}$, and thus the average of K is given by $\langle K \rangle = 2\pi \chi_{\mathrm{IPMS}}/S_{\mathrm{IPMS}}$. It has been shown that the quantity $\langle K^2 \rangle / \langle K \rangle^2 = 1.2187$ for all three minimal surfaces [57]. The dimensionless surface area σ_{IPMS} per unit cell, of volume V_{IPMS}, is given by $\sigma_{\mathrm{IPMS}} = S_{\mathrm{IPMS}}/V_{\mathrm{IPMS}}^{2/3}$, and has values 2.4177, 2.3451 and 2.4537 for D, P and G, respectively. This shows that the G surface is the most compact, and the P surface is the least compact, for a given value of surface area S per unit cell.

However, for the conventional crystallographic unit cells of the cubic phases $Pn3m$, $Im3m$ and $Ia3d$, based respectively on the D, P and G minimal surfaces, the values of g, χ and σ are different. The reason for this is that, although for the $Im3m$ cubic phase, the P minimal surface and the $Im3m$ cubic phase unit cells are the same, *this is not the case* for the other two cubic phases. The $Pn3m$ cubic phase unit cell has *half* the volume of the D-surface unit cell, and the $Ia3d$ cubic phase has *twice* the volume of the G surface unit cell. If the underlying minimal surfaces of these cubic phases are related by the Bonnet transformation, which gives a one-to-one mapping of all surface patches on the minimal surfaces, then the cubic phase lattice parameters, given by $a = V^{1/3} = (S/\sigma)^{1/2}$, should have a fixed relationship to each other, as shown in the last column of table 4.

Another noteworthy difference between these phases is their porosity, which is a gauge of the number of water channels that split off each junction. The gyroid phase is the least porous, with three vertices, while the double-diamond and primitive have four and six vertices, respectively. Theoretical predictions of the observed swelling behaviour of the three $\mathrm{Q_{II}}$ phases [72], which depend on the geometric characteristics given in table 4, have been found to agree closely with experimental results, as can be seen in figure 9.

For co-existing bicontinuous cubic phases, the unit cell dimensions are predicted to satisfy the Bonnet ratios given in table 4 (a/a_{Pn3m}), and this has been observed experimentally [76]. Bonnet ratios have also been noted during transitions between inverse bicontinuous cubic phases [15].

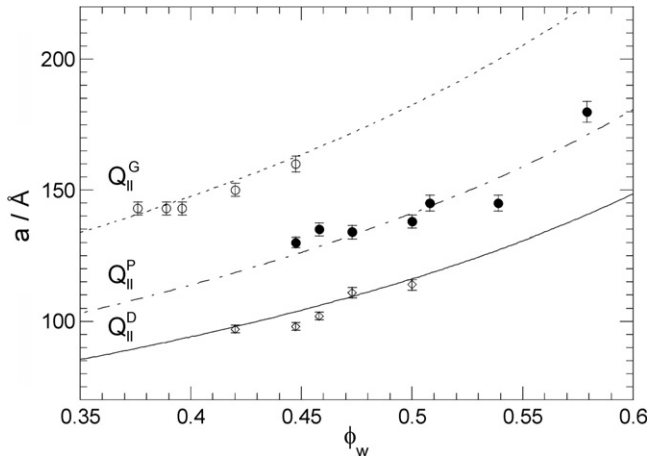

Figure 9. Theoretical fits to the observed swelling of the lattice parameters of the three cubic phases $Ia3d$, $Pn3m$ and $Im3m$ of the 2:1 lauric acid/dilauroylphosphatidylcholine system for a parallel surface model. From [72].

The Helfrich ansatz was developed using an initial assumption that the lipid bilayer could be modelled as an infinitely thin sheet. An incompatibility occurs when considering the inverse bicontinuous cubic phases, where the 'thin sheet' lies over the minimal surface. By definition, the mean curvature, H, for a minimal surface is zero and, remembering that for symmetric bilayers the spontaneous mean curvature, H_0, is also zero, the Helfrich ansatz can be simplified to $g_c = \kappa_G^b K$, i.e. the curvature elastic energy is proportional to the Gaussian curvature (remembering that we are considering the curvature elasticity of the bilayer, hence κ_G^b). Since the Gaussian curvature K is dependent on the lattice dimensions, the curvature elastic energy can be reduced by simply decreasing the lattice size. Therefore, minimization of the curvature elastic energy would try to make the lattice parameter indefinitely small. Obviously, this is not realized in reality, which implies that the Helfrich ansatz breaks down when the radii of curvature are of a similar magnitude to the thickness of the lipids. Such considerations have led to an extension of the Helfrich equation by Ljunggren and Eriksson [45], discussed briefly in section 2. Physical effects, such as transverse interactions, have also been proposed to stabilize the inverse bicontinuous cubic phases at a preferred lattice parameter. For uncharged lipids, transverse interactions such as hydration repulsion are significant only for low water volume fractions, but may dominate for charged lipids, since electrostatic repulsions act over long range and therefore high water volume fractions.

2.6. Constant mean curvature versus parallel interfaces

The three Q_{II} phases can be depicted as bilayers draped over triply periodic minimal surfaces. It has been suggested [77] that the two monolayers could either form *parallel surfaces* (to the underlying minimal surface) or *constant mean curvature (CMC) surfaces*, or possibly an intermediate situation between the two extremes. A parallel surface can be defined when the extension of a normal from any point on the parallel surface to the minimal surface is always equidistant. This does not hold true for constant mean curvature surfaces, for which, by inference, the mean curvature is equal over the entire pivotal surface. In comparison, the pivotal surface of the H_{II} phase lies on both the CMC and the parallel surface simultaneously.

Most models developed to investigate the Q_{II} phases are based on the parallel surface model, which is a reasonable assumption for very swollen phases. However, the contribution from the CMC surface should not be overlooked. The curvature elasticity of the three bicontinuous cubic phases has been modelled for both the CMC and the parallel interfaces [12]. Templer *et al* found that there was an energetic degeneracy for the parallel interface model, which would lead to all three of the bicontinuous cubic phases existing together, a condition that has not been found experimentally. The model for the pivotal surface having a constant mean curvature was found to break the degeneracy, where the sequence for an increasing water volume fraction was given by G → D → P, which is the same sequence observed both experimentally for 2LA/DLPC (figure 8) and also predicted by Schwarz and Gompper [71].

3. Packing frustration

The total free energy of a lipid–water system consists of three factors: the curvature elasticity; an energetic term representing various interaction forces; and also an energy relating to the packing of the hydrocarbon chains, generally known as the *packing frustration*. It has been recognized in the last few years that the packing frustration inherent in the curved inverse lipid phases may have a larger energetic contribution than previously thought, and preliminary experiments have been undertaken to characterize its effect. Contiguously, theoretical models have been developed, initially by Anderson *et al* [77, 78], and extended by Templer *et al* [11, 12].

A simple concept, frequently used in the field of inorganic chemistry to rationalize why some structures, e.g. cubic close-packing (ccp), are adopted by certain elements, is that of the 'packing fraction' of a system, which calculates the volume occupied by the spherical elements, where the remainder is empty space. This idea can be extended to the curved inverse phases formed by the packing of aggregates of amphiphilic molecules, and some packing fractions have been estimated [79]. Treating the phases as close packings of idealized inverse circular cylinders or inverse spheres allows the fraction of potential 'void' volume to be estimated. The void volume has to be uniformly filled, either by some of the hydrocarbon chains of the amphiphiles deviating from their preferred conformational states in order to reach into the voids, or by partitioning of added non-polar molecules such as alkanes into the void regions. The packing fraction for the inverse hexagonal phase is $\pi/\sqrt{12} \approx 0.91$ (9% void volume), whereas for the $Fd3m$ inverse micellar cubic phase the packing fraction is 0.71 (29% void volume), corresponding to a much higher degree of packing frustration. However, this simple approach does not give the whole answer, since a simple face-centred cubic (fcc) packing of identical spheres would have a packing fraction of 0.74, i.e. would apparently be slightly less frustrated than the $Fd3m$ phase, and yet such simple fcc inverse cubic phases are never seen, whereas the $Fd3m$ phase is now known to be quite common.

3.1. Modelling the packing frustration

The inverse hexagonal phase has a quite high degree of packing frustration, caused by the geometric packing of circular cylinders not being able to fill space completely. This results in 'voids', as shown in figure 10.

The lipid hydrocarbon chains must stretch or compress away from their preferred conformation to compensate and fill the hydrophobic cavities, giving an energy penalty. The requirement that, for inversely curved phases, the hydrocarbon chains have to deform leads to the conclusion that there must be a swelling limit for each phase. The argument follows

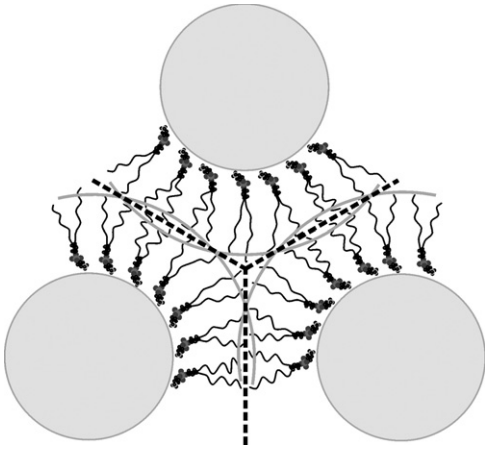

Figure 10. The packing frustration within the H_{II} phase, where the hydrocarbon chains must stretch or compress to fill the void regions.

that, for greater lattice parameters, the voids must also inherently be larger, and therefore the chains must extend further to avoid a vacuum being created. At some large lattice parameter, the chains will be forced to extend to their limit, as given by their all-*trans* configuration. No further lengthening is physically possible and, since empty space must be filled, the lipid system must have reached its swelling limit, and will be forced to adopt a different phase.

The models developed to evaluate the packing frustration in a lipid system all estimate the energy constrained in the variation of the hydrocarbon chain extension from the relaxed state, l_r, for each amphiphile. The chains have been assumed to act as harmonic springs, so the energy tied-up in the packing frustration can be expressed simply as a function of the stretching rigidity of the chains, k, and the monolayer width at some point on the interface, l:

$$g_P = k\,(l - l_r)^2\,. \tag{9}$$

This crude model has been extended to construct expressions for the packing frustration of the inverse hexagonal phase as well as the three bicontinuous cubic phases. The H_{II} phase was found to have a much higher packing cost than any of the three bicontinuous cubics, but a lower curvature elastic energy [12, 77]. These computations may also serve to explain some observations that have been widely noted, but not definitively recorded and rationalized. One such rule of thumb is that Q_{II} phases tend to be found for diacyl or dialkyl phospholipids that have chain lengths of C_{14} or shorter. The reasoning behind this is that longer hydrocarbon chains can relieve packing frustration, which would encourage the formation of the H_{II} phase, whereas the shorter chain lengths are unable to extend easily to fill the voids, and so the inverse bicontinuous cubic phases, with lower packing frustration, dominate. For example, the C_{14} ether-linked ditetradecylphosphatidylethanolamine (DTPE)/water system exhibits a direct L_α–H_{II} transition, whereas the corresponding C_{12} (DDPE)/water system has extensive regions of cubic phase existence [5]. Pressure has been shown to be able to induce Q_{II} phases for the C_{14} (DTPE)/water system [64], where an increase in pressure forces the hydrophobic chains to pack closer together, which inhibits the filling of the void regions, and induces a phase change first into a bicontinuous cubic structure, before the H_{II} phase appears at higher temperature.

3.2. Experimental results showing the effect of packing frustration

The addition of an alkane to a lipid/water system in order to relieve packing stress was a tool used by Rand [54] and others to be able to examine the curvature elasticity independently. Equally, however, the packing frustration inherent for a system can also be examined by the amount of hydrophobic moiety needed to relieve it. A detailed study of the effect of the progressive addition of an alkane to the monoacylglyceride 1-monoolein by Khoo *et al* [80] has shown that, under certain conditions, the system is able to go through a series of phase changes, from $Q_{II} \rightarrow H_{II} \rightarrow Fd3m \rightarrow L_2$. The relief of packing frustration by the alkane was allowing the formation of phases with increasingly inverse interfacial curvature.

Interestingly, although the $Fd3m$ phase has so far not been observed for pure phospholipid/water systems, there have been examples of its existence in the phase diagrams of purely binary glycolipid/water mixtures [81]. Again, longer chain lengths favour the phase with a higher packing frustration. Somewhat speculative arguments have been put forward to explain why glycolipids appear to be able to adopt phases that are too frustrated for phospholipid systems. The adoption of the $Fd3m$ phase by a binary amphiphile/water system is a peculiar phenomenon. The structure of the phase was shown earlier to be very distinctive, with each unit cell consisting of eight large inverse micelles and sixteen smaller inverse micelles, packed in a regular arrangement. Assuming that the packing frustration is relieved to some degree either by long chain lengths or the addition of a hydrophobic molecule, the desire to relieve curvature will eventually drive the system to form spherical micelles. Curiously, the $Fd3m$ phase has two different sizes of inverse micelle, which will lead to intrinsic curvature issues. One would therefore expect a structure such as the face-centred cubic (fcc) structure to be adopted preferentially, since it has a very similar packing fraction to that of the $Fd3m$ phase. However, the shapes of the voids also need to be considered, as well as the packing fraction. The empty spaces are spread relatively evenly throughout the unit cell of an $Fd3m$ phase, which implies that, although a high percentage of the chains need to depart away from their preferred conformation, the variation in chain extension is quite low. In contrast, the empty spaces in the fcc lattice are fewer but deeper, i.e. the chains in contact with the voids must, on average, have a longer chain length than those for the $Fd3m$ phase. Consideration of the energetics relating to the variance in chain extension of these two phases leads to the conclusion that the $Fd3m$ phase is favoured.

4. Summary

In this paper we have discussed the inverse phases commonly adopted by lipids found in biological membranes, where these range from the well-characterized phospholipids to glycolipids and monoglycerides. The inverse phases generally recognized and focused on here are the H_{II}, Q_{II} and $Fd3m$ phases, although we note in passing that there seems to be no reason why *inverse* curved 'liquid-ordered' phases should not occur in lipids with a tendency for inverse curvature, upon addition of sterols. A liquid-ordered inverse bicontinuous cubic phase will be quite difficult to distinguish from its more usual fluid version, since the wide-angle x-ray pattern, and presumably the NMR spectra, will be very similar. Nevertheless, we expect that such phases will be discovered in the near future. We have given an overview of the energetics that determine the phase behaviour of lipid/water systems and our current understanding of the competition between the curvature elasticity and packing frustration, focusing on the inverse bicontinuous cubic phases in section 2. A good appreciation of the relationship between cell membrane curvature and many biological processes, including intracellular trafficking, is becoming increasingly important, and an insight into the driving forces behind membrane curvature is vital.

Acknowledgments

We thank the UK Engineering and Physical Sciences Research Council (EPSRC) for the award of Platform grant GR/S77721. We are also grateful to our past and present collaborators, and members of the Liquid Crystals and Membrane Biophysics group at Imperial College London, for their invaluable contributions.

References

[1] Seddon J M and Templer R H 1993 Cubic phases of self-assembled amphiphilic aggregates *Phil. Trans. R. Soc.* A **344** 377–401
[2] Seddon J M and Templer R H 1995 Polymorphism of lipid–water systems *Handbook of Biological Physics* ed R Lipowsky and E Sackmann (Amsterdam: Elsevier Science B.V., North-Holland) pp 97–160
[3] Templer R H 1998 Thermodynamic and theoretical aspects of cubic mesophases in nature and biological amphiphiles *Curr. Opin. Colloid Interface Sci.* **3** 255–63
[4] Seddon J M 1996 Lyotropic phase behaviour of biological amphiphiles *Ber. Bunsenges. Phys. Chem.* **100** 380–93
[5] Seddon J M 1990 Structure of the inverted hexagonal (H_{II}) phase, and non-lamellar phase-transitions of lipids *Biochim. Biophys. Acta* **1031** 1–69
[6] Seddon J M, Templer R H, Warrender N A, Huang Z, Cevc G and Marsh D 1997 Phosphatidylcholine fatty acid membranes: effects of headgroup hydration on the phase behaviour and structural parameters of the gel and inverse hexagonal (H-II) phases *BBA—Biomembranes* **1327** 131–47
[7] Seddon J M, Robins J, Gulik-Krzywicki T and Delacroix H 2000 Inverse micellar phases of phospholipids and glycolipids *Phys. Chem. Chem. Phys.* **2** 4485–93
[8] Templer R H, Seddon J M and Warrender N A 1994 Measuring the elastic parameters for inverse bicontinuous cubic phases *Biophys. Chem.* **49** 1–12
[9] Templer R H 1995 On the area neutral surface of inverse bicontinuous cubic phases of lyotropic liquid-crystals *Langmuir* **11** 334–40
[10] Templer R H, Turner D C, Harper P and Seddon J M 1995 Corrections to some models of the curvature elastic energy of inverse bicontinuous cubic phases *J. Physique* II **5** 1053–65
[11] Duesing P M, Templer R H and Seddon J M 1997 Quantifying packing frustration energy in inverse lyotropic mesophases *Langmuir* **13** 351–9
[12] Templer R H, Seddon J M, Duesing P M, Winter R and Erbes J 1998 Modelling the phase behavior of the inverse hexagonal and inverse bicontinuous cubic phases in 2:1 fatty acid phosphatidylcholine mixtures *J. Phys. Chem.* B **102** 7262–71
[13] Templer R H, Khoo B J and Seddon J M 1998 Gaussian curvature modulus of an amphiphilic monolayer *Langmuir* **14** 7427–34
[14] Vacklin M, Khoo B J, Madan K H, Seddon J M and Templer R H 2000 The bending elasticity of 1-monoolein upon relief of packing stress *Langmuir* **16** 4741–8
[15] Squires A M *et al* 2005 Kinetics and mechanism of the interconversion of inverse bicontinuous cubic mesophases *Phys. Rev.* E **72** 011502
[16] Conn C E *et al* 2006 Dynamics of structural transformations between lamellar and inverse bicontinuous cubic lyotropic phases *Phys. Rev. Lett.* **96** 108102
[17] Seddon J M *et al* 2006 Pressure-Jump x-ray studies of liquid crystal transitions in lipids *Phil. Trans. R. Soc.* A at press
[18] Jahn R and Grubmuller H 2002 Membrane fusion *Curr. Opin. Cell Biol.* **14** 488–95
[19] Hyde S T *et al* 1997 *The Language of Shape* (Amsterdam: Elsevier Science B.V.)
[20] Epand R M (ed) 1997 *Current Topics in Membranes: Lipid Polymorphism and Membrane Properties* (New York: Academic)
[21] Dubois-Violette E and Pansu B (ed) Colloque de Physique *Int. Workshop on Geometry and Interfaces (Aussois, France, 1990)* Les Editions de Physique
[22] McMahon H T and Gallop J L 2005 Membrane curvature and mechanisms of dynamic cell membrane remodelling *Nature* **438** 590–6
[23] Zimmerberg J and Kozlov M M 2006 How proteins produce cellular membrane curvature *Natl Rev. Mol. Cell Biol.* **7** 9–19
[24] Holthuis J C M 2004 Regulating membrane curvature *Topics in Current Genetics* ed S Keränen and J Jäntti (Heidelberg: Springer GmbH) pp 39–64
[25] Balasubramanian K and Schroit A J 2003 Aminophospholipid asymmetry: a matter of life and death *Annu. Rev. Physiol.* **65** 701–34

[26] Lynch M L and Spicer P T (ed) 2005 *Bicontinuous Liquid Crystals* (Boca Raton, FL: Taylor and Francis)
[27] Landau E M and Rosenbusch J P 1996 Lipidic cubic phases: a novel concept for the crystallization of membrane proteins *Proc. Natl Acad. Sci.* **93** 14532–5
[28] Caffrey M 2003 Membrane protein crystallization *J. Struct. Biol.* **142** 108–32
[29] Sennoga C, Heron A, Seddon J M, Templer R H and Hankamer B 2003 Membrane-protein crystallization in cubo: temperature-dependent phase behaviour of monoolein-detergent mixtures *Acta Crystallogr.* D **59** 239–46
[30] Drummond C J and Fong C 2000 Surfactant self-assembly objects as novel drug delivery vehicles *Curr. Opin. Colloid Interface Sci.* **4** 449–56
[31] Chesnoy S and Huang L 2000 Structure and function of lipid–DNA complexes for gene delivery *Annu. Rev. Biophys. Biomol. Struct.* **29** 27–47
[32] Ewert K K, Ahmad A, Evans H M and Safinya C R 2005 Cationic lipid–DNA complexes for non-viral gene therapy: relating supramolecular structures to cellular pathways *Expert Opin. Biol. Th.* **5** 33–53
[33] Luzzati V 1968 X-ray diffraction studies of lipid–water systems *Biological Membranes* ed D Chapman (London: Academic) pp 71–123
[34] Mariani P, Luzzati V and Delacroix H 1988 Cubic phases of lipid-containing systems-structure-analysis and biological implications *J. Mol. Biol.* **204** 165–88
[35] Luzzati V, Vargas R, Gulik A, Mariani P, Seddon J M and Rivas E 1992 Lipid polymorphism: a correction. The structure of the cubic phase of extinction symbol Fd—consists of two types of disjointed reverse micelles embedded in a three-dimensional hydrocarbon matrix *Biochemistry* **31** 279–85
[36] Scriven L E 1976 Equilibrium bicontinuous structure *Nature* **263** 123–5
[37] Gozdz W T and Holyst R 1996 Triply periodic surfaces and multiply continuous structures from the Landau model of microemulsions *Phys. Rev.* E **54** 5012–27
[38] Matsen M W and Bates F S 1996 Unifying weak- and strong-segregation block copolymer theories *Macromolecules* **29** 1091–8
[39] Hyde S T, Andersson S, Ericsson B and Larsson K 1984 A cubic structure consisting of a lipid bilayer forming an infinite periodic minimum surface of the gyroid type in the glycerolmonooleat-water system *Z. Kristallogr.* **168** 213–9
[40] Israelachvili J 1992 *Intermolecular and Surface Forces* (Santa Barbara, CA: Academic)
[41] Kumar V V 1991 Complementary molecular shapes and additivity of the packing parameter of lipids *Proc. Natl Acad. Sci.* **88** 444–8
[42] Kirk G L, Gruner S M and Stein D L 1984 A thermodynamic model of the lamellar to inverse hexagonal phase-transition of lipid-membrane water-systems *Biochemistry* **23** 1093–102
[43] Helfrich W 1973 Elastic properties of lipid bilayers—theory and possible experiments *Z. Naturf.* c **28** 693–703
[44] Helfrich W 1981 Amphiphilic mesophases made of defects *Physics of Defects (Les Houches, 1980)* ed R Balian, M Kleman and J P Poirer (Amsterdam: North-Holland) pp 713–56
[45] Ljunggren S and Eriksson J C 1992 Minimal-surfaces and Winsor III microemulsions *Langmuir* **8** 1300–6
[46] Helfrich W 1981 Amphiphilic mesophases made of defects *Physics of Defects* ed R Balian, M Kleman and J P Poirer (Amsterdam: North-Holland) p 713
[47] Bowie J U 2005 Solving the membrane protein folding problem *Nature* **438** 581–9
[48] Booth P J, Templer R H, Curran A R and Allen S J 2001 Can we identify the forces that drive the folding of integral membrane proteins? *Biochem. Soc. Trans.* **29** 408–13
[49] Hong H D and Tamm L K 2004 Elastic coupling of integral membrane protein stability to lipid bilayer forces *Proc. Natl Acad. Sci.* **101** 4065–70
[50] Kozlov M M and Winterhalter M 1991 Elastic-moduli for strongly curved monolayers—position of the neutral surface *J. Physique* II **1** 1077–84
[51] Leikin S L, Kozlov M M, Fuller N L and Rand R P 1996 Measured effects of diacylglycerol on structural and elastic properties of phospholipid membranes *Biophys. J.* **71** 2623–32
[52] Kirk G L and Gruner S M 1985 Lyotropic effects of alkanes and headgroup composition on the $L\alpha$–HII lipid liquid crystal phase transition: hydrocarbon packing versus intrinsic curvature *J. Physique* **46** 761–9
[53] Rand R P, Fuller N and Chen Z S 1998 Measuring spontaneous curvature and bending moduli of membrane lipid layers *Biophys. J.* **74** A27
[54] Rand R P, Fuller N L, Gruner S M and Parsegian V A 1990 Membrane curvature, lipid segregation, and structural transitions for phospholipids under dual-solvent stress *Biochemistry* **29** 76–87
[55] Gruner S M, Parsegian V A and Rand R P 1986 Directly measured deformation energy of phospholipid HII hexagonal phases *Faraday Discuss.* **81** 29–37
[56] Siegel D P and Kozlov M M 2004 The Gaussian curvature elastic modulus of N-monomethylated dioleoylphosphatidylethanolamine: relevance to membrane fusion and lipid phase behavior *Biophys. J.* **87** 366–74

[57] Helfrich W and Rennschuh H 1990 Landau theory of the lamellar-to-cubic phase-transition *J. Physique Coll.* **51** C7189–95
[58] Chen Z and Rand R P 1997 The influence of cholesterol on phospholipid membrane curvature and bending elasticity *Biophys. J.* **73** 267–76
[59] Méléard P, Gerbeaud C, Bardusco P, Jeandaine N, Mitov M D and Fernandez-Puente L 1998 Mechanical properties of model membranes studied from shape transformations of giant vesicles *Biochimie* **80** 401–13
[60] Lee C H, Lin W C and Wang J P 2001 All-optical measurements of the bending rigidity of lipid-vesicle membranes across structural phase transitions *Phys. Rev.* E **6402** 020901
[61] Otten D, Brown M F and Beyer K 2000 Softening of membrane bilayers by detergents elucidated by deuterium NMR spectroscopy *J. Phys. Chem.* B **104** 12119–29
[62] Schwarz U S and Gompper G 2001 Bending frustration of lipid–water mesophases based on cubic minimal surfaces *Langmuir* **17** 2084–96
[63] Squires A M, Templer R H and Seddon J M 2002 Models and measurements on the monolayer bending energy of inverse lyotropic mesophases *Biophys. Chem. (Imperial College London, UK, 2001)* ed R H Templer and R Leatherbarrow (Cambridge: The Royal Society of Chemistry) pp 177–90
[64] Duesing P M, Seddon J M, Templer R H and Mannock D A 1997 Pressure effects on lamellar and inverse curved phases of fully hydrated dialkyl phosphatidylethanolamines and beta-D-xylopyranosyl-sn-glycerols *Langmuir* **13** 2655–64
[65] Winter R *et al* 1999 Inverse bicontinuous cubic phases in fatty acid/phosphatidylcholine mixtures: the effects of pressure and lipid composition *Phys. Chem. Chem. Phys.* **1** 887–93
[66] Niggemann G, Kummrow M and Helfrich W 1995 The bending rigidity of phosphatidylcholine bilayers: dependences on experimental method, sample cell sealing and temperature *J. Physique* II **5** 413–25
[67] Epand R M, Epand R F, Decicco A and Schwarz D 2000 Curvature properties of novel forms of phosphatidylcholine with branched acyl chains *Eur. J. Biochem.* **267** 2909–15
[68] Kawabata Y *et al* 2004 Temperature and pressure effects on the bending modulus of monolayers in a ternary microemulsion *Phys. Rev. Lett.* **92** 1–4
[69] Kozlov M M, Leikin S L and Markin V S 1989 Elastic properties of interfaces *J. Chem. Soc. Faraday Trans.* II **85** 277–92
[70] Larsson K 1989 Cubic lipid–water phases: structures and biomembrane aspects *J. Phys. Chem.* **93** 7304–14
[71] Schwarz U S and Gompper G 2000 Stability of inverse bicontinuous cubic phases in lipid–water mixtures *Phys. Rev. Lett.* **85** 1472–5
[72] Templer R H *et al* 1998 Inverse bicontinuous cubic phases in 2:1 fatty acid phosphatidylcholine mixtures. The effects of chain length, hydration, and temperature *J. Phys. Chem.* B **102** 7251–61
[73] Engblom J and Hyde S T 1995 On the swelling of bicontinuous lyotropic mesophases *J. Physique* II **5** 171–90
[74] Fischer W and Koch E 1987 On 3-periodic minimal surfaces *Z. Kristallogr.* **179** 31–2
[75] Hyde S T 1992 Interfacial architecture in surfactant water mixtures—beyond spheres, cylinders and planes *Pure Appl. Chem.* **64** 1617–22
[76] Tenchov B, Koynova R and Rapp G 1998 Accelerated formation of cubic phases in phosphatidylethanolamine dispersions *Biophys. J.* **75** 853–66
[77] Anderson D M, Gruner S M and Leibler S 1988 Geometrical aspects of the frustration in the cubic phases of lyotropic liquid-crystals *Proc. Natl Acad. Sci.* **85** 5364–8
[78] Anderson D M, Davis H T, Scriven L E and Nitsche J C C 1990 Periodic surfaces of prescribed mean-curvature *Adv. Chem. Phys.* **77** 337–96
[79] Hyde S T 2001 Identification of lyotropic liquid crystalline mesophases *Handbook of Applied Surface and Colloid Chemistry* ed K Holmberg (New York: Wiley) pp 299–332
[80] Khoo B J 1996 *An Experimental Examination of Ideas in the Curvature Elasticity of Lyotropic Liquid Crystals* (London: Imperial College)
[81] Seddon J M, Zeb N, Templer R H, McElhaney R N and Mannock D A 1996 An $Fd3m$ lyotropic cubic phase in a binary glycolipid/water system *Langmuir* **12** 5250–3